Available online at www.sciencedirect.com
SCIENCE DIRECT®
PERGAMON
International Journal of Heat and Mass Transfer 46 (2003) 3777–3787
International Journal of HEAT and MASS TRANSFER
www.elsevier.com/locate/ijhmt

# Effect of inlet flow maldistribution on the thermal performance of a three-fluid crossflow heat exchanger

Ping Yuan *

*Department of Mechanical Engineering, Lee-Ming Institute of Technology, No. 2-2, Lee Zhuan Road, Taishan, Taipei, Taiwan, ROC*

Received 25 October 2002; received in revised form 4 April 2003

**Abstract**

This study investigates the effect of flow maldistribution on the thermal performance of a three-fluid crossflow heat exchanger by the numerical method. In the inlets of three fluid streams, this study considers four modes of flow nonuniformity arrangement by using three flow maldistribution models. According to the results of temperature fields, effectiveness and deterioration factor, this study discusses the deterioration or promotion due to the flow maldistribution in the heat exchanger. The results indicate that there is a best one in choice between the four maldistribution modes and the best flow maldistribution mode promotes the thermal performance of a three-fluid crossflow heat exchanger when NTU and heat capacity rate ratios are large.


## 1. Introduction

Three-fluid heat exchangers are widely used in cryogenics and chemical processes, such as separation of air, purification and liquefaction of hydrogen. In addition, a three-fluid stream heat exchanger may be desirable or even necessary due to space constraints in industry. In modern applications, the design and construction of micromechanical components and devices might involve heat exchange between more than two fluids as in the case of a microcompact heat exchanger. The intelligent arrangement of three fluid streams in crossflow is that one stream with highest or lowest temperature flows through the center layer sandwiched between the other two streams, as shown in Fig. 1. Much research has focused on the analysis of thermal performance of a three-fluid crossflow heat exchanger. Willis and Chapman [1] predict the performance of a single-pass, three-fluid crossflow heat exchanger by the numerical method and the performance is presented graphically in terms of the temperature effectiveness of two of the fluids. Baclic et al. [2] obtain the exact solution to the exit mean temperature of each fluid in a three-fluid crossflow heat exchanger using Laplace transformation. Sekulic and Kmecko [3] derive an expression for overall effectiveness to provide insight into the overall performance of three-fluid heat exchangers. Sekulic and Shah [4] introduce a comprehensive review of three-fluid heat exchangers and also provide a detailed description of the crossflow arrangement. In addition, Yuan and Kou [5] investigate the effect of longitudinal wall conduction in a three-fluid crossflow heat exchanger by the numerical method.

In the inlets of a heat exchanger, the fluid flow distribution over the heat exchanger core is usually not uniform under actual operating conditions. The flow nonuniformity through the heat exchanger is generally associated with improper headers and distributors. Chiou [6] investigates the deterioration of the heat exchanger effectiveness due to flow nonuniformity on one side of a crossflow heat exchanger. Chiou [7] discusses the effect of longitudinal heat conduction and the flow nonuniformity on the thermal performance of a two-fluid crossflow heat exchanger. Ranganayakulu et al. [8] uses a finite element model to analyze the effects of nonuniform inlet fluid flow distribution on both hot and cold fluid sides of a crossflow plate-fin compact heat exchanger. Lalot et al. [9] presents the effect of flow nonuniformity on the performance of heat exchangers,

* Tel.: +886-2-29097811x2230; fax: +886-2-22966301.
*E-mail address:* pyuan@mail.lit.edu.tw (P. Yuan).

0017-9310/03/$ - see front matter © 2003 Elsevier Ltd. All rights reserved.
doi:10.1016/S0017-9310(03)00196-0

**Nomenclature**

| | |
|---|---|
| $a$ | total heat transfer area |
| $C$ | heat capacity rate |
| $C^*$ | heat capacity rate ratio, as defined in Eq. (7) |
| $G$ | mass flow velocity |
| $h$ | convection heat transfer coefficient |
| $L$ | length of the crossflow heat exchanger with subscript $x$ or $y$ |
| $\dot{m}$ | mass flow rate |
| $N$ | dimensionless parameter, as defined in Eq. (7) |
| NTU | number of transfer units, as defined in Eq. (7) |
| $T$ | dimensionless temperature, as defined in Eq. (7) |
| $T'$ | temperature |
| $\overline{T}$ | mean temperature |
| $x$ | coordinate in the $x$ direction |
| $X$ | dimensionless coordinate in the $x$ direction, $x/L_x$ |
| $y$ | coordinate in the $y$ direction |
| $Y$ | dimensionless coordinate in the $y$ direction, $y/L_y$ |
| $\alpha$ | local flow nonuniformity parameter, as defined in Eq. (7) |
| $\beta$ | a constant such as $h \sim G^{\beta}$ |
| $\varepsilon$ | effectiveness of a three-fluid heat exchanger, as defined in Eq. (8) |
| $\eta$ | total surface efficiency, dimensionless |
| $\tau$ | deterioration factor, as defined in Eq. (9) |

*Subscripts*

| | |
|---|---|
| 1 | fluid 1 |
| 2 | fluid 2 |
| 21 | portion of fluid 2 near fluid 1 |
| 23 | portion of fluid 2 near fluid 3 |
| 3 | fluid 3 |
| a | dividing wall a |
| b | dividing wall b |
| e | exit |
| i | inlet |
| $x$ | $x$ direction |
| $y$ | $y$ direction |

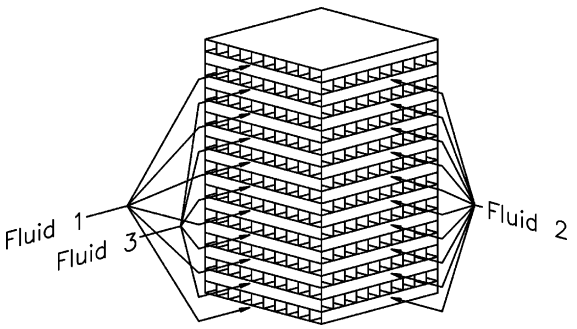


Fig. 1. A three-fluid crossflow heat exchanger core.

based on the study of flow maldistribution in an experimental electrical heater. The results indicate that the flow maldistribution leads to a loss of effectiveness of about 25% for crossflow exchangers. Using finite element method, Ranganayakulu and Seetharamu [10] investigate the effects of longitudinal wall conduction, nonuniform inlet fluid flow and nonuniform inlet temperature distribution on the thermal performance of a two-fluid crossflow plate-fin heat exchanger.

According to the previous study, the effect of flow maldistribution on the thermal performance of a two-fluid crossflow heat exchanger is detrimental and not neglected. However, to our knowledge, there has been little literature focusing on the analysis of flow maldistribution effect in a three-fluid crossflow heat exchanger. Because of the complicated arrangement of three fluid streams in a three-fluid crossflow heat exchanger, the optimal design and manufacture of headers and distributors still generate the nonuniform inlet fluid flow. Therefore, the effect of flow maldistribution on the thermal performance of a three-fluid crossflow heat exchanger must be considered. Using finite difference method, this study investigates the effect of flow maldistribution on the thermal performance of a three-fluid crossflow heat exchanger.

## 2. Governing equations and mathematical formulation

The following analysis presents a method for determining the exit mean temperatures of one unit in a three-fluid crossflow heat exchanger, as shown in Fig. 2. In this study, certain idealizations derived from Shah and Sekulic [11] are as follows:

1. The heat exchanger operates under steady state conditions.
2. Heat losses to the surroundings are negligible.
3. There are no heat generation, phase change, longitudinal wall conduction and viscous dissipation within the fluid streams.

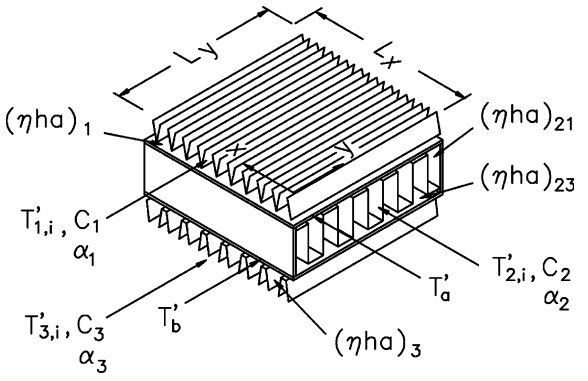


Fig. 2. Schematic diagram of crossflow heat exchanger units.

4. In the inlets of each fluid stream, the temperature distribution is constant with respect to time and position.
5. The thermal–physical properties of all fluid streams and dividing walls are constant and uniform.
6. The individual convection heat transfer coefficient between each fluid stream and the respective heat transfer surface of the dividing wall is directly proportional to the mass velocity of the fluid flow, or $h \sim G^{\beta}$.

In Fig. 2, the fluid stream with the highest or lowest temperature is selected as the central fluid stream. Because heat is transferred from the central fluid stream 2 to each outer fluid streams 1 and 3 respectively, there is no heat transferred directly between the two outer fluid streams. The $x$ coordinate direction is chosen in the direction of fluid stream 2 and $y$ is chosen in the direction of fluid streams 1 and 3. The application of energy conservation leads to the following five simultaneous, dimensionless partial differential equations.

$$N_1\alpha_1^{\beta}(T_a - T_1) = \alpha_1\frac{\partial T_1}{\partial Y} \tag{1}$$

$$N_{21}\alpha_2^{\beta}(T_a - T_2) + N_{23}\alpha_2^{\beta}(T_b - T_2) = \alpha_2\frac{\partial T_2}{\partial X} \tag{2}$$

$$N_3\alpha_3^{\beta}(T_b - T_3) = \alpha_3\frac{\partial T_3}{\partial Y} \tag{3}$$

$$N_{21}\alpha_2^{\beta}(T_2 - T_a) + N_1\alpha_1^{\beta}C_1^*(T_1 - T_a) = 0 \tag{4}$$

$$N_{23}\alpha_2^{\beta}(T_2 - T_b) + N_3\alpha_3^{\beta}C_3^*(T_3 - T_b) = 0 \tag{5}$$

The inlet conditions are

$$\begin{cases} T_1(X,0) = 0 \\ T_2(0,Y) = 1 \\ T_3(X,0) = T_{3,i} \end{cases} \tag{6}$$

The dimensionless parameters are defined as:

$$T = \frac{T' - T'_{1,i}}{T'_{2,i} - T'_{1,i}}, \quad X = \frac{x}{L_x}, \quad Y = \frac{y}{L_y}, \quad C_1^* = \frac{C_1}{C_2},$$

$$C_3^* = \frac{C_3}{C_2}, \quad \alpha = \frac{\dot{m}_{\text{local}}}{\dot{m}_{\text{average}}},$$

$$N_1 = \frac{(\eta ha)_1}{C_1}, \quad N_{21} = \frac{(\eta ha)_{21}}{C_2}, \quad N_{23} = \frac{(\eta ha)_{23}}{C_2},$$

$$N_3 = \frac{(\eta ha)_3}{C_3},$$

$$\text{NTU} = \left[C_1\left(\frac{1}{(\eta ha)_{21}} + \frac{1}{(\eta ha)_1}\right)\right]^{-1} \tag{7}$$

## 3. Computational details

This study divides each domain of fluid streams 1, 2 and 3, walls a and b into the same $N \times N$ subdivisions, as shown in Fig. 3. Along the flow direction of fluid streams 1 and 3, $T_{1(i,j)}, T_{3(i,j)}$ and $T_{1(i+1,j)}, T_{3(i+1,j)}$ are specified in the inlet and exit of the subdivisions. Similarly, along the flow direction of fluid stream 2, $T_{2(i,j)}$ and $T_{2(i,j+1)}$ are specified in the inlet and exit of the subdivision. The nodes of $T_{a(i,j)}$ and $T_{b(i,j)}$ are assigned in the center of the subdivisions. The governing equations can be discretized individually into finite difference equations by means of this grid generation. In addition, this study divides the front area of each fluid stream into $10 \times 10$ cells in order to fit the inlet nonuniformity models cited from the literature by Chiou [7]. They are 10 subdivisions in $x$ or $y$ direction crossing 10 subdivisions in stacking direction. It is noted that each front area cell may include many layers in stacking direction and calculating subdivisions in $x$ or $y$ direction. Each front area cell has the local flow nonuniformity parameter, $\alpha$, and

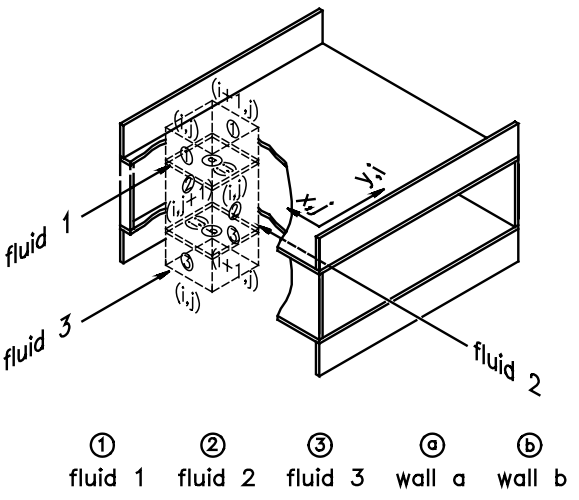


Fig. 3. Subdivision of crossflow heat exchanger units.

the summation of $\alpha$ over the front area is one. The procedures of the numerical calculation are (1) Calculate the temperature fields of each fluid stream in iteration step $n$ from the finite difference equation, respectively. (2) Use the temperatures of fluid streams obtained from Step 1 to solve the temperature field of the dividing wall in iteration step $n$ using the finite difference equation of the wall. (3) Treat the results of Step 2 as the updated values. Return to Step 1 and repeat the whole procedure until the total sum of each grid point's absolute error between two consecutive iterations in each temperature field is less than 0.01. (4) Repeat the procedure of Steps 1–3 to calculate the temperature field in next stacking subdivision until all stacking subdivisions are done. (5) Calculate the exit mean temperatures of each fluid stream in this heat exchanger. The size of calculating subdivision depends on the value of NTU and $C^*$. In this study, the subdivision size is from $10 \times 10$ when $C_1^* = C_3^* = 0.5$ and NTU $= 0.1$ to $100 \times 100$ when $C_1^* = C_3^* = 1.0$ and NTU $= 10$. Fig. 4 shows the comparison between the present numerical solution and Chiou's [7] solution. In this case of comparison, this study considers that the three-fluid crossflow heat exchanger has balance flow and the inlet temperature of fluid stream 3 is zero. Hence, the three-fluid crossflow heat exchanger is identical to a two-fluid crossflow heat exchanger. In addition, this comparison case considers the flow maldistribution is on one side of the exchanger core and uniform flow is on another side. Clearly, the results in this study agree with the previous results in Fig. 4, so this numerical method is reliable.

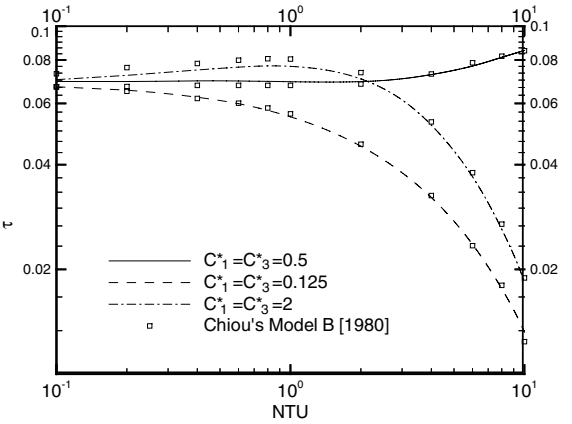


(a) Chiou's[7] Model B

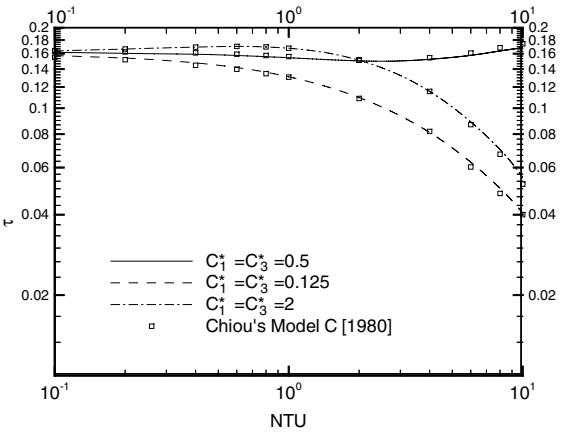


(b) Chiou's[7] Model C

Fig. 4. Comparison of deterioration factor in this study and previous study when Chiou's model B or model C is on the side of fluid stream 2 and uniform flow is on the side of fluid streams 1 and 3.

## 4. Results and discussion

This study selects the value of parameters as NTU $= 0.1$–$10$, $C_1^* = 0.5$ and 1.0, $C_3^* = 0.5$ and 1.0, as well as $T_{3,i} = 0.0$ and 0.5. Fig. 5 shows the profiles of inlet flow nonuniformity considered by this study. They are cited from models B and C in the literature of Chiou [7]. These models are obtained directly from wind tunnel experiments. According to the schematic diagram of flow arrangement in Fig. 1, this study selects the models C, A and B as the inlet flow maldistribution of fluid streams 1, 2 and 3, respectively. This study uses Mode CAB to represent this arrangement of flow maldistribution in the heat exchanger. When the positions of inlet duct of fluid streams 1 and 3 changes with each other, the arrangement of flow maldistribution becomes to Mode BAC. In addition, this study considers $\beta$ is 0.0 and 0.8 in the fully developed laminar flow and turbulence flow.

Fig. 6 shows the isotherm of fluid stream 2 at the exit for different arrangements of flow maldistribution when NTU $= 2$, $C_1^* = C_3^* = 0.5$, $T_{3,i} = 0$ and $\beta = 0.8$. Meanwhile, Modes UUU and AAA represent the inlet flow maldistribution of each fluid stream is uniform and Model A, respectively. In Fig. 6(a), the isotherm is straight line and the temperature increases from 0 to 0.5 along the $y$ direction when all inlet flows are uniform. When the inlet flow is Mode AAA, the isotherm in the central stacking subdivisions approaches to right at $Y < 0.5$ and to left at $Y > 0.5$. This means the temperature in the central stacking subdivisions is lower than that in up and down stacking subdivisions at $Y < 0.5$ and higher than that at $Y > 0.5$. Because the intelligent design is to select the fluid stream with the highest or lowest temperature as the center fluid stream, heat is transferred between the center fluid stream 2 and each outer fluid streams 1 and 3. There is no heat directly transferred between the two outer fluid streams. Therefore, the enthalpy change of fluid stream 2 from inlet to

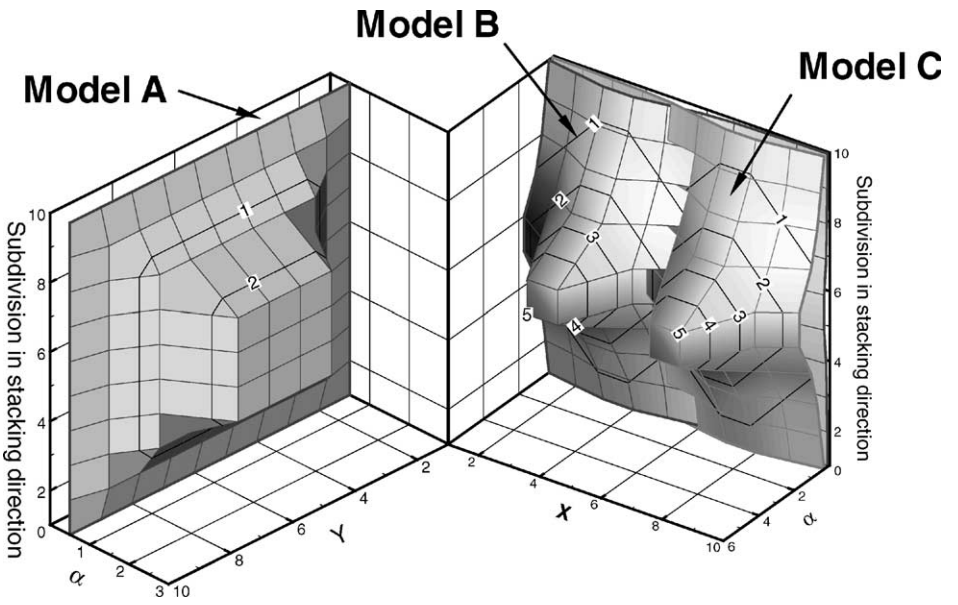


Fig. 5. Flow maldistribution models.

exit represents the overall thermal performance of a three-fluid crossflow heat exchanger. Because the mass flow rate in the center of front area at Mode AAA is higher than that at Mode UUU and the shift to left of isotherm is more than the shift to right of isotherm, the enthalpy change of fluid stream 2 from inlet to exit at Mode AAA is lower than that at Mode UUU. Consequently, the thermal performance in Mode AAA is lower than that in Mode UUU. Fig. 6(c) and (d) depict the isotherm of exit temperature of fluid stream 2 in Modes CAB and BAC, respectively. Because both inlet temperature of fluid streams 1 and 3 are zero, the Mode CAB is identical to Mode BAC. Therefore, the isotherm in Mode CAB is same to that in Mode BAC. In the two figures, it is obvious that the overall temperature in Modes CAB and BAC is higher than that in Modes UUU and AAA.

Fig. 7 depicts the isotherm of fluid stream 2 at the exit with same conditions to Fig. 6 except the inlet temperature of fluid stream 3 is 0.5. Comparing Fig. 7(a) and (b), it indicates that the isotherm in the central stacking subdivisions approaches to right at $Y < 0.5$ and to left at $Y > 0.5$. This phenomena is similar to the results in Fig. 6(a) and (b). However, the temperature increases rapidly at the portion of $Y$ nearing 0.15, where is close to the inlet of fluid streams 1 and 3. This means the temperature of fluid stream 2 occurs jump at this portion. Fig. 7(c) and (d) depicts the isotherm of exit temperature of fluid stream 2 in Modes CAB and BAC, respectively. Comparing the two figures indicates that the temperature jump at $Y$ nearing 0.15 in Mode CAB is lower than that in Mode BAC. Hence, the overall exit temperature in Mode CAB is predicted to be lower that that in Mode BAC. Because the flow maldistribution of fluid stream 2 is Model A in both Modes CAB and BAC. The temperature difference between inlet and exit of fluid stream 2 indicates the enthalpy change between inlet and exit. This means the thermal performance of a three-fluid heat exchanger in Mode CAB should be better than that in Mode BAC. Fig. 8 shows all exit temperature profile of fluid stream 2 at four maldistribution modes with same conditions to those in Fig. 7. In this figure, the shape of profile at Mode AAA is similar to that at Mode UUU in most top and bottom stacking subdivisions, but the shape in central stacking subdivisions at Mode AAA is higher than that at Mode UUU. The shape of profile at $Y > 0.5$ in Mode CAB is similar to that in Mode BAC, but the temperature at $Y < 0.5$ in Mode CAB is lower obviously than that in Mode BAC. Comparing the four profiles implicates that the exit mean temperature of fluid steam 2 is in a descent order of Modes BAC, CAB, AAA and UUU. Because the enthalpy change of fluid stream 2 from inlet to exit represents the overall heat exchange of a three-fluid crossflow heat exchanger, this study considers that the thermal performance in the four inlet flow modes are in a descent order of Modes UUU, AAA, CAB and BAC.

Fig. 9 shows that the temperature profiles of fluid stream 2 flowing through stacking subdivision 5 at Modes UUU, CAB and BAC when $\mathrm{NTU} = 10$, $C_1^* = C_3^* = 0.5$, $T_{3,i} = 0.5$ and $\beta = 0.8$. When the inlet flow is uniform, the temperature of fluid stream 2 decreases smoothly from inlet temperature of 1.0 and the

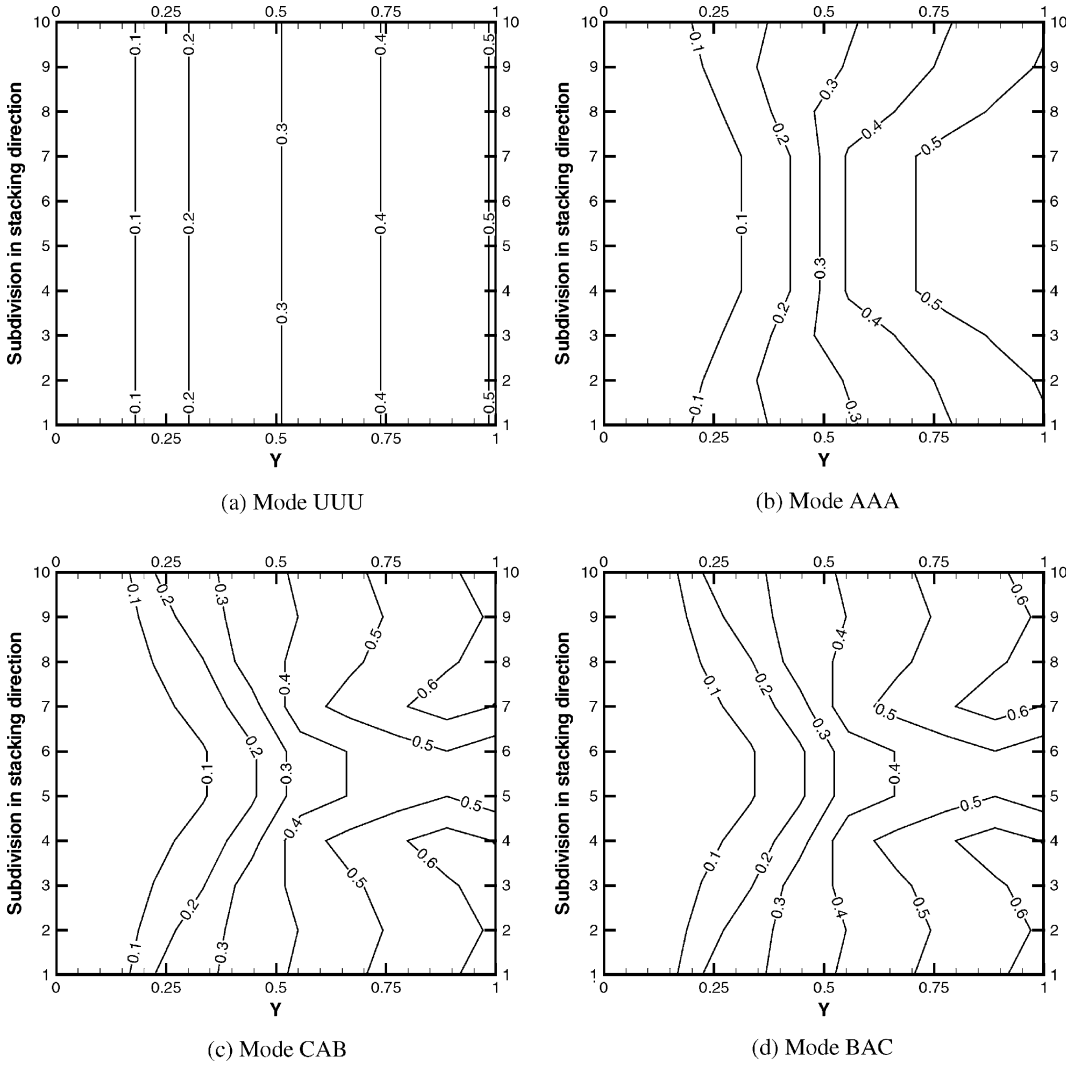


Fig. 6. Isotherm of fluid stream 2 at the exit when NTU = 2, $C_1^* = C_3^* = 0.5$, $T_{3,i} = 0$ and $\beta = 0.8$.

temperature at the portion closing to the inlet of fluid streams 1 and 3 is lower than that at portion closing to the exit of fluid streams 1 and 3. When the flow maldistribution is Mode CAB, the temperature drop is more than that in uniform flow. Because the temperature profile shown in this figure is focused on stacking subdivision 5, which is the central subdivision of a heat exchanger core in the stacking direction, the mass flow velocity of each fluid stream has the maximum in this stacking subdivision at Mode CAB. Therefore, the temperature difference of fluid stream 2 from inlet to exit at Mode CAB is larger than that at Mode UUU in this central stacking subdivision. If we inspect the temperature in up and down subdivision in stacking direction, the temperature difference of fluid stream 2 from inlet to exit at Mode CAB should be lower than that in uniform flow. When the inlet flow maldistribution is Mode BAC, the phenomenon of unexpected heat exchange has happened. In Fig. 9(c), at the portion nearing the inlet of fluids 1 and 3, the temperature of fluid stream 2 decrease steeply to a minimum of 0.2 and then increase to the exit temperature about 0.4. Obviously, the fluid stream 2 at $Y < 0.5$ transfers heat to both fluids 1 and 3 at the zone of $0 < X < 0.5$, but absorbs heat from fluid 3 at the zone of $0.5 < X < 1$. The inlet ducts position of Mode CAB is shown in Fig. 1 and the inlet ducts position of Mode BAC is changing the duct positions of fluids 1 and 3 in Fig. 1. According to the schematic diagram of flow arrangement in Fig. 1, the fluid streams 3 and 1 exchange heat mainly with fluid stream 2 at the first half core and the last half core of a heat exchanger respectively, although the fluid stream 2 exchanges heat simultaneously

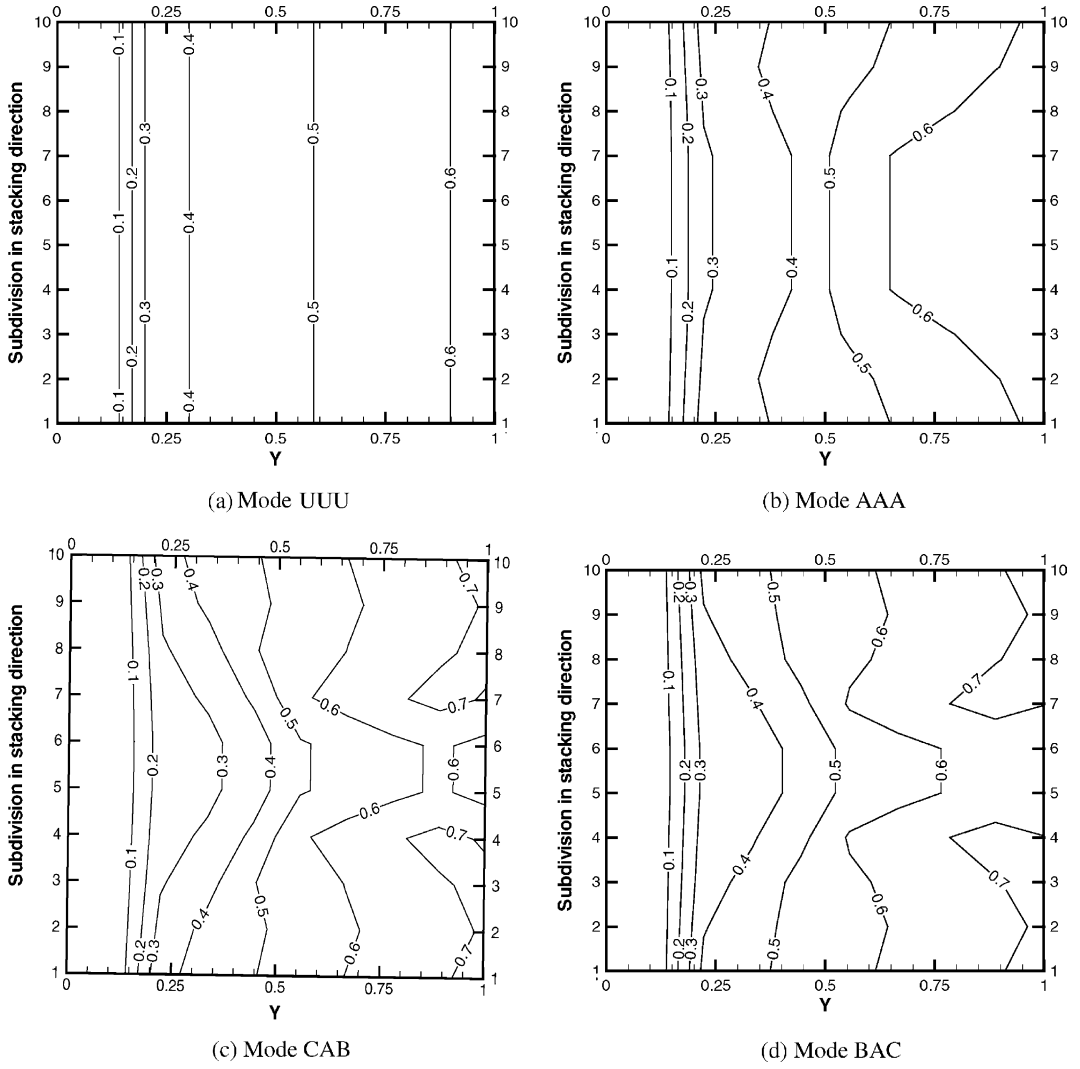


Fig. 7. Isotherm of fluid stream 2 at the exit when NTU = 2, $C_1^* = C_3^* = 0.5$, $T_{3,i} = 0.5$ and $\beta = 0.8$.

with fluids 1 and 3. Oppositely, at Mode BAC, the fluid streams 1 and 3 exchanges heat mainly with fluid stream 2 at the first half core and the last half core of a heat exchanger, respectively. This situation induces the temperature of fluid stream 2 to drop more at the first half core especially in the area close to the inlet of fluids 1 and 3. Therefore, the fluid stream 2 flowing through the last half core absorbs heat from fluid stream 3 with inlet temperature of 0.5. The phenomenon of transferring heat out and in at fluid stream 2 is waste. Moreover, the process of heating fluid stream 2, which has the highest inlet temperature, is unexpected in a heat exchanger. Therefore, the Mode BAC is the worst.

According to the definition of the effectiveness of a three-fluid heat exchanger by Sekulic and Kmecko [3],

$$\varepsilon = \frac{C_1^* \overline{T}_{1,e} + C_3^* (\overline{T}_{3,e} - T_{3,i})}{C_1^* + C_3^* (1 - T_{3,i})} \tag{8}$$

this study compares the thermal performance at different flow maldistribution to each other in Fig. 10. This figure shows the effectiveness versus NTU at $C_1^* = C_3^* = 0.5$, $T_{3,i} = 0.5$ and $\beta = 0.8$. Obviously, all effectiveness at different flow maldistribution increases when NTU increases. This is reasonable because of the relationship between effectiveness and NTU in heat exchanger. In addition, the descending order of effectiveness is Modes UUU, AAA, CAB and BAC when NTU < 4. Nevertheless, when NTU > 4, the effectiveness at Modes AAA and CAB are higher than that at Mode UUU. In the research about the effect of inlet flow nonuniform on a two-fluid heat exchanger, the results of Chiou [6] show

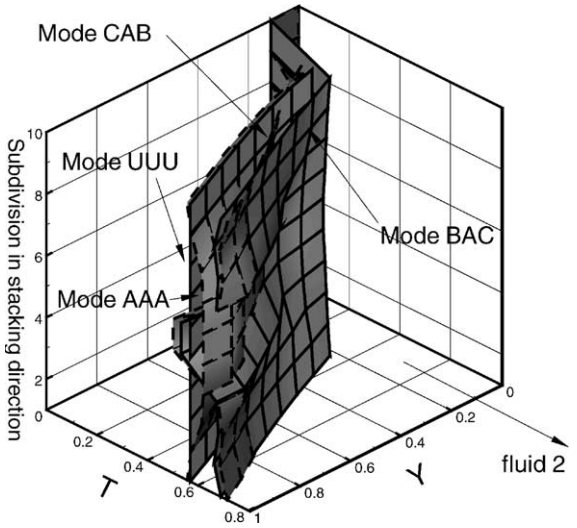


Fig. 8. Exit temperature profile of fluid stream 2 when NTU = 2, $C_1^* = C_3^* = 0.5$, $T_{3,i} = 0.5$ and $\beta = 0.8$.

that the effect of nonuniform flow decrease the effectiveness of a heat exchanger. The results in Fig. 10 show that the effectiveness at some flow maldistribution is higher than that in uniform flow in a three-fluid crossflow heat exchanger when NTU is large and $\beta$ is 0.8.

In order to discuss detail about the effect of maldistribution on the thermal performance of a three-fluid crossflow heat exchanger, this study defines the deterioration factor due to the flow maldistribution as follows:

$$\tau = \frac{\varepsilon_{\text{uniform}} - \varepsilon_{\text{nonuniform}}}{\varepsilon_{\text{uniform}}} \tag{9}$$

Fig. 11 shows the deterioration factor in different modes versus NTU at $C_1^* = C_3^* = 0.5$, $T_{3,i} = 0.0$ and 0.5, as well as $\beta = 0.8$. In this figure, the continuous line and dashed line represent the deterioration factor at $T_{3,i} = 0.0$ and 0.5, respectively. It is obvious that the continuous lines coincide with each other between Modes BAC and CAB, because the thermal and fluid conditions are identical when the inlet temperature of fluid stream 3 is zero. In addition, the continuous line and dashed line coincide with each other in Mode AAA, because the effectiveness and deterioration factor are not affected by the change of inlet temperature of fluids under same thermal and fluid conditions. When the inlet temperature of fluid stream 3 increases from 0.0 to 0.5, the deterioration factor of Modes BAC and CAB move up and down, respectively. This means the deterioration factor of Mode CAB is lower than that of Mode BAC when the inlet temperature of fluid stream 3 is not zero. Consequently, the deterioration factor in a three-fluid heat exchanger is in ascending order of Modes AAA, CAB and BAC. Although the Mode AAA is the best one, the

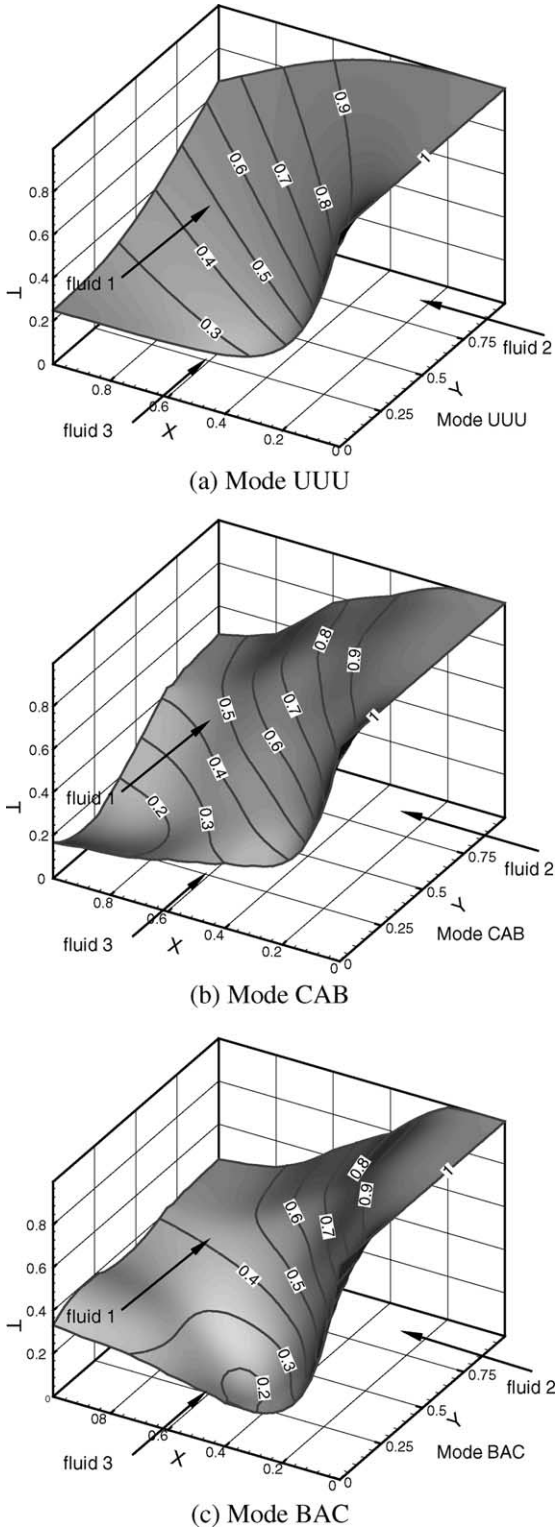


Fig. 9. Temperature profiles of fluid stream 2 on stacking subdivision 5 at Modes UUU, CAB and BAC when NTU = 10, $T_{3,i} = 0.5$ and $\beta = 0.8$.

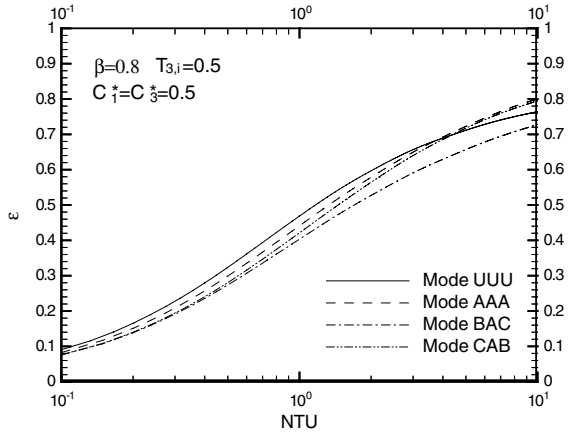


Fig. 10. Effectiveness versus NTU at different inlet flow mode when $C_1^* = C_3^* = 0.5$, $\beta = 0.8$ and $T_{3,i} = 0.5$.

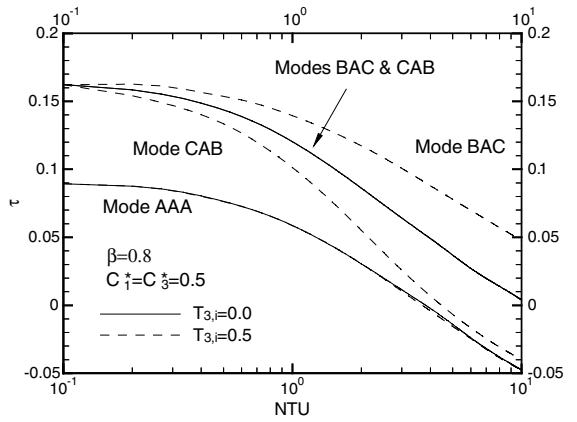


Fig. 11. Deterioration factor in different modes versus NTU at $C_1^* = C_3^* = 0.5$, $\beta = 0.8$, as well as $T_{3,i} = 0.0$ and 0.5.

arrangement of this mode is hard to apply in practical industry. Therefore, the Mode CAB has good priority in application to industry. Comparing the deterioration factor of Modes BAC and CAB in this figure shows that the difference of deterioration factor between Modes CAB and BAC is from 0% at NTU = 0.1 to 10% at NTU = 10 when $T_{3,i} = 0.5$. Therefore, the right arrangement of inlet flow is important to a three-fluid crossflow heat exchanger. In other words, the inlet duct of fluid stream 3 should be located at the first half core along the flow direction of fluid stream 2, as shown in Fig. 1. In addition, it is worth to note that the deterioration factor decreases to negative at Modes AAA and CAB when NTU > 4. This means that the effect of inlet flow maldistribution promotes the thermal performance of a three-fluid crossflow heat exchanger in this case. Chiou [7] had stated that when flow maldistribution occur on both fluid sides, the deterioration of the exchanger performance may be greater or less than when only one fluid side is nonuniformly distributed. According to the result in Fig. 11, this study wants to extend the statement to that when flow maldistribution occur on three fluid sides, the exchanger performance may be greater or less than when all fluid side is uniformly distributed.

Fig. 12 shows the deterioration factor in different heat capacity rate ratio versus NTU at Mode CAB, $\beta = 0.8$, as well as $T_{3,i} = 0.0$ and 0.5. Comparing the deterioration factor at $C_1^* = C_3^* = 0.5$, as well as $C_1^* = 0.5$ and $C_3^* = 1.0$ indicates that the deterioration factor increases below 3% with the increase of heat capacity rate ratio of fluid stream 3. Comparing the deterioration factor at $C_1^* = 0.5$ and $C_3^* = 1.0$, as well as $C_1^* = C_3^* = 1.0$ indicates that the deterioration factor decreases below 10% with the increase of heat capacity rate ratio of fluid stream 1. Consequently, the deterioration factor is affected slightly by the increase of heat capacity rate ratio of fluid stream 3, but severely by the increase of heat capacity rate ratio of fluid stream 1 when the flow is in turbulent mode. In this figure, the deterioration factor decreases to negative at $C_1^* = C_3^* = 1.0$ and $T_{3,i} = 0.5$ when the NTU increases more than 1. This means the maldistribution Mode CAB promotes the thermal performance of a three-fluid crossflow heat exchanger when both heat capacity rate ratios and NTU are more than 1.

Fig. 13 depicts the effectiveness versus NTU at different inlet flow mode when $C_1^* = C_3^* = 0.5$, $T_{3,i} = 0.5$ and $\beta = 0.0$. The continuous line, dashed line, dash-dotted line and dash-double-dotted line represent the Modes UUU, AAA, BAC and CAB, respectively. In this figure, the descending order of effectiveness is Modes UUU, AAA, CAB and BAC for all NTU. Because the arrangement of Modes UUU and AAA are impossible in industry application, the Mode CAB has good

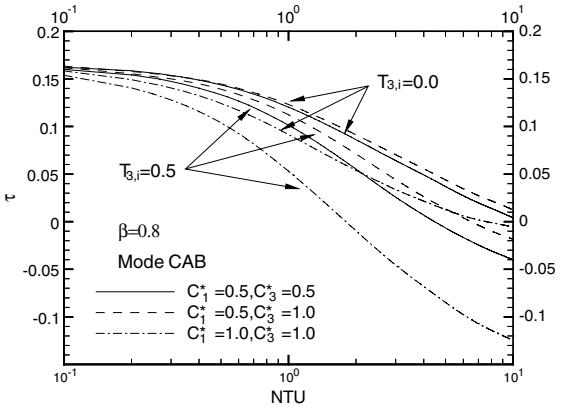


Fig. 12. Deterioration factor in different heat capacity rate ratio versus NTU at Mode CAB, $\beta = 0.8$, as well as $T_{3,i} = 0.0$ and 0.5.

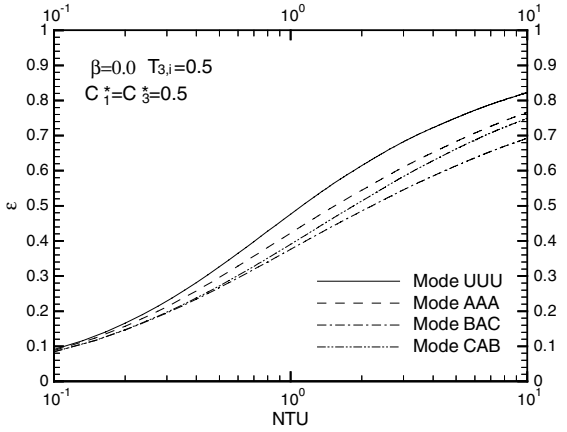


Fig. 13. Effectiveness versus NTU at different inlet flow mode when $C_1^* = C_3^* = 0.5$, $T_{3,i} = 0.5$ and $\beta = 0.0$.

priority in the inlet flow maldistribution when the channel flow is considered as laminar. The result is agreeable with the previous result in turbulent flow. Therefore, no matter the flow is in laminar or turbulent mode, the inlet duct of fluid 3 should be put in the first half core and inlet duct of fluid 1 should be put in the last half core in a three-fluid crossflow heat exchanger, as shown in Fig. 1. Fig. 14 shows that the deterioration factor versus NTU at Modes AAA, BAC and CAB when $C_1^* = C_3^* = 0.5$, $T_{3,i} = 0.0$ and 0.5, as well as $\beta = 0.0$. In this figure, the deterioration factor at Mode AAA is the lowest and the deterioration factor at Mode BAC is higher than that at Mode CAB when inlet temperature of fluid stream 3 is not zero. Therefore, the thermal performance at different maldistribution modes in laminar flow is in the same descending order to that in turbulent flow. In contrast to Fig. 11, the deterioration factor does not increase continuously with the increase of NTU, but it increases to a maximum when NTU is close to 1 and then decrease when the NTU increases continuously. In this figure, the range of maximum deterioration factor is between 10% and 20%. In addition, the deterioration factor at Mode CAB is above 10% when $0.2 < \mathrm{NTU} < 8$. Therefore, the deterioration due to flow maldistribution is not neglected in laminar flow.

Fig. 15 depicts the deterioration factor in different heat capacity rate ratio versus NTU at Mode CAB, $\beta = 0$, as well as $T_{3,i} = 0.0$ and 0.5. In this figure, the decrease of deterioration factor from continuous line to dashed line is below 5% when the heat capacity rate ratio of fluid stream 3 increases from 0.5 to 1.0. The decrease of deterioration factor from dashed line to dash-dotted line is below 9% when the heat capacity rate ratio of fluid stream 1 increases from 0.5 to 1.0 at $\mathrm{NTU} > 1$, but the deterioration factor increases slightly when the heat capacity rate ratio of fluid stream 1 increases from 0.5 to 1.0 at $\mathrm{NTU} < 1$. Even the increase of NTU or heat capacity rate ratio reduces the deterioration due to the flow maldistribution, the value of deterioration factor in laminar flow is still more than 10% when $0.2 < \mathrm{NTU} < 8$ at $C_1^* = C_3^* = 0.5$, as well as $0.2 < \mathrm{NTU} < 4$ at $C_1^* = 0.5$ and $C_3^* = 1.0$. When the maldistribution is in turbulent flow, the deterioration factor decrease continuously with the increase of NTU and the value of deterioration factor reduce to below 10% when $C_1^* = C_3^* = 0.5$ in Fig. 12. Therefore, the effect of flow maldistribution on the thermal performance of a three-fluid crossflow heat exchanger in laminar flow is more severely than that in turbulent flow when the heat capacity rate ratios are small. According to the results in Figs. 12 and 15, the deterioration of thermal performance is not neglected in laminar flow when

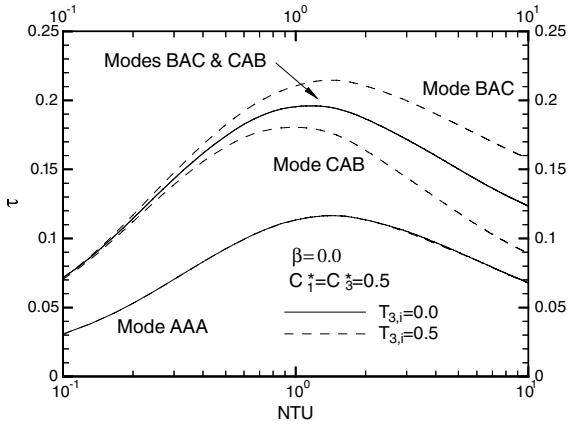


Fig. 14. Deterioration factor versus NTU at Modes AAA, BAC and CAB when $C_1^* = C_3^* = 0.5$, $T_{3,i} = 0.0$ and 0.5, as well as $\beta = 0.0$.

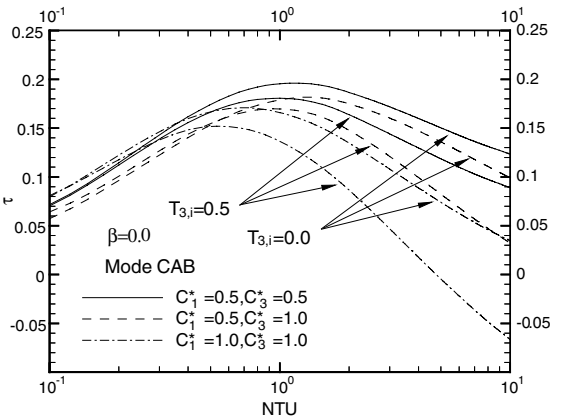


Fig. 15. Deterioration factor in different heat capacity rate ratio versus NTU at Mode CAB, $\beta = 0$, as well as $T_{3,i} = 0.0$ and 0.5.

$0.1 < \mathrm{NTU} < 10$ and in turbulent flow when $\mathrm{NTU} < 2$ at the Mode CAB.

## 5. Conclusions

This study investigates the effect of flow maldistribution on the thermal performance of a three-fluid crossflow heat exchanger. Using the definition of effectiveness and deterioration factor, this study discusses the deterioration or promotion of thermal performance due to the maldistribution in the heat exchanger at flow maldistribution Modes UUU, AAA, CAB and BAC. According to the above discussion, this study has some conclusions: (1) The thermal performance at these four maldistribution modes is in a descending order of Modes UUU, AAA, CAB, and BAC in most cases, but the thermal performance at Modes AAA and CAB is higher than that at Mode UUU in some cases. In other words, when flow maldistribution occurs on three fluid sides, the exchanger performance may be greater or less than when all fluid side in uniformly distributed. (2) The thermal performance at Mode BAC is the worst, because fluid stream 2 happens the unexpected heat exchange with fluid streams 1 and 3. In addition, the flow maldistribution Mode CAB is the best one in the application to industry. (3) The deterioration factor decreases with the increase of inlet temperature of fluid stream 3 at Mode CAB and it increases with the increase of inlet temperature of fluid stream 3 at Mode BAC. The difference of deterioration factor between Modes CAB and BAC is above 10% in large NTU, so the suitable selection of inlet duct position of fluid streams 1 and 3 is important. (4) The deterioration factor affected by the increase of heat capacity rate ratio of fluid stream 1 is more severely than by the increase of heat capacity rate ratio of fluid stream 3. (5) The effectiveness promotion at Mode CAB is more with larger NTU and larger heat capacity rate ratios. (6) The effectiveness deterioration at Mode CAB is not negligible at small heat capacity rate ratios when $\mathrm{NTU} < 2$ in turbulent flow and when $0.1 < \mathrm{NTU} < 10$ in laminar flow.

## References

[1] N.C. Willis, A.J. Chapman, Analysis of three-fluid, crossflow heat exchanger, ASME Journal of Heat Transfer 90 (1968) 333–339.
[2] B.S. Baclic, D.P. Sekulic, D.D. Gvozdenac, Performances of three-fluid single pass crossflow heat exchanger, in: Heat Transfer 1982, Hemisphere, Washington DC, 1982, pp. 167–172.
[3] D.P. Sekulic, I. Kmecko, Three-fluid heat exchanger effectiveness-revisited, ASME Journal of Heat Transfer 117 (1995) 226–229.
[4] D.P. Sekulic, R.K. Shah, Thermal design theory of three-fluid heat exchangers, Advanced Heat Transfer 26 (1995) 219–328.
[5] P. Yuan, H.S. Kou, The effect of longitudinal wall conduction in a three-fluid crossflow heat exchanger, Numerical Heat Transfer Part A—Applications 34 (1998) 135–150.
[6] J.P. Chiou, Thermal performance deterioration in crossflow heat exchanger due to the flow nonuniformity, ASME Journal of Heat Transfer 100 (1978) 580–587.
[7] J.P. Chiou, The advancement of compact heat exchanger theory considering the effects of longitudinal heat conduction and flow nonuniformity, in: R.K. Shah, C.F. McDonald, C.P. Howard (Eds.), Compact Heat Exchangers—History, Technological Advancement and Mechanical Design Problems, American Society of Mechanical Engineers, New York, 1980, pp. 101–121.
[8] Ch. Ranganayakulu, K.N. Seetharamu, K.V. Sreevatsan, The effects of inlet fluid flow nonuniformity on thermal performance and pressure drops in crossflow plate-fin compact heat exchangers, International Journal of Heat and Mass Transfer 40 (1997) 27–38.
[9] S. Lalot, P. Florent, S.K. Lang, A.E. Bergles, Flow maldistribution in heat exchangers, Applied Thermal Engineering 19 (1999) 847–863.
[10] Ch. Ranganayakulu, K.N. Seetharamu, The combined effects of longitudinal heat conduction flow nonuniformity and temperature nonuniformity in crossflow plate-fin heat exchangers, International Communication in Heat and Mass Transfer 26 (1999) 669–678.
[11] R.K. Shah, D.P. Sekulic, Heat exchangers, in: W.M. Rohsenow, J.P. Hartnett, Y.I. Cho (Eds.), Handbook of Heat Transfer, McGraw-Hill, New York, 1998, pp. 17.27–17.28.